Advances in Geo-Energy Research

Vol. 3, No. 4, p. 396-409, 2019

Original article

# Comparison of multi-field coupling numerical simulation in hot dry rock thermal exploitation of enhanced geothermal systems

Shichao Chen[1], Bin Ding[1], Liang Gong[1]*, Zhaoqin Huang[2], Bo Yu[3], Shuyu Sun[4]

[1]*College of New Energy, China University of Petroleum (East China), Qingdao 266580, P. R. China*

[2]*School of Petroleum Engineering, China University of Petroleum (East China), Qingdao 266580, P. R. China*

[3]*Beijing Key Laboratory of Pipeline Critical Technology and Equipment for Deepwater Oil and Gas Development, Beijing Institute of Petrochemical Technology, Beijing 102617, P. R. China*

[4]*Computational Transport Phenomena Laboratory (CTPL), King Abdullah University of Science and Technology (KAUST), Thuwal, 23955-6900, Kingdom of Saudi Arabia*

(Received December 1, 2019; revised December 12, 2019; accepted December 12, 2019; available online December 14, 2019)

**Citation:**
Chen, S., Ding, B., Gong, L., Huang, Z., Yu, B., Sun, S. Comparison of multi-field coupling numerical simulation in hot dry rock thermal exploitation of enhanced geothermal systems. *Advances in Geo-Energy Research*, 2019, 3(4): 396-409, doi: 10.26804/ager.2019.04.07.

**Corresponding author:**
*E-mail: lgong@upc.edu.cn

**Keywords:**
Numerical simulation
TH coupling
THM coupling
THMC coupling
comparative analysis

**Abstract:**
In order to alleviate the environmental crisis and improve energy structure, countries from all over the world have focused on the hot dry rock geothermal resources with great potential and with little pollution. The geothermal heat production from enhanced geothermal system comes with complex multi-field coupling process, and it is of great significance to study the temporal and spatial evolution of geothermal reservoir. In this work, a practical numerical model is established to simulate the heat production process in EGS, and the comparison of thermal-hydraulic (TH), thermal-hydraulic-mechanical (THM) and thermal-hydraulic-mechanical-chemical (THMC) coupling in geothermal reservoir is analyzed. The results show that the stable production stage of the three cases is approximately 5 years; however, compared with TH and THMC coupling, the service-life for THM coupling decreased by 1140 days and 332 days, respectively. The mechanical enhanced effects are offset by the chemical precipitation, and the precipitation from $SiO_2$ is much larger than the dissolution of calcite.

## 1. Introduction

In recent years, with the growing global energy crisis and environmental problems, geothermal resources have aroused greatly interests around the world due to its cleanness, reproducibility, stability and large abundance of storage (Liu et al., 2018, 2019). Geothermal resources can be divided into hydro-thermal and hot dry rock (HDR) resources, and majority of the heat energy is stored in the HDR geothermal resources (Chen et al., 2019). According to reported statistics, the total HDR resource reserve in the continental area of China within 3-10 km depth is $2.5 \times 10^{25}$ J (equivalent to energy contained in $856 \times 10^{12}$ t standard coal), and the basic resource reserve buried above 5.5 km are about $3.1 \times 10^{24}$ J (China Geological Survey, 2018). However, the HDR reservoir is dense and nearly impervious, making it difficult to extract stored thermal energy by traditional techniques. The enhanced or engineered geothermal system (EGS) creates an artificial heat reservoir by hydraulic fracturing processes to economically extract heat energy from low permeability and porosity geothermal resources, which has been widely used to develop HDR resources (Han et al., 2019; Wei et al., 2019).

Extraction of heat from an EGS reservoir involves several coupled processes in the fractured rock mass, including the thermal process, hydraulic process, mechanical process and chemical process, which are generally termed as thermal-hydraulic-mechanical-chemical (THMC) coupling. The spatial evolution of these multi-physical processes is complex and

https://doi.org/10.26804/ager.2019.04.07.

affected by a large number of parameters. Therefore, this plays a crucial role to study and compare individual (thermal-hydraulic (TH), thermal-hydraulic-mechanical (THM)) and combined THMC effects for the performance of heat extraction.

In terms of multi-field coupling, Zeng et al. (2013) investigated the HDR thermal exploitation potential of TH coupling process in the Desert Peak geothermal field in American through a single vertical and horizontal well. The results indicate that desirable heat production efficiency can be attained under suitable fracture permeability and water production rate. Ijeje et al. (2019) successfully implemented the fully implicit coupled simulator TFReact with the consideration of THM coupling to evaluate the influence of anisotropic thermal drawdown in triggering permeability evolution. Analysis shows that low anisotropic permeability values will lead to late cold water breakthrough at producer, slower migration rate and wider sweep area than high anisotropic permeability values. Huang et al. (2015) developed an efficient parallel fully-coupled thermal-hydro-mechanical simulator to model $CO_2$ transport in porous media. The results show that there are several characteristics can be used to detect $CO_2$ leakage pathways. A numerical approach is presented by Sun et al. (2017) to simulate and analyze the heat extraction process in EGS, and an EGS case from Cooper Basin, Australia is simulated with 2D stochastically generated fracture model to study the characteristics of fluid flow, heat transfer and mechanical response in geothermal reservoir. The results show the significance of taking into account the THM coupling effects when investigating the efficiency and performance of EGS.

However, the effect of chemical reaction on the hydraulic properties of the rock fractures and the spatial distribution of the fracture network is overlooked in these studies. For a better understanding of the performance of EGS, Ogata et al. (2018) developed a multi-physics numerical model to predict the fluid flow and mass transport behavior of rock fractures under coupled THMC conditions. Through the comparison of experiment and simulation calculation, the developed model should be valid for evaluating the evolution in the fluid flow and mass transport behavior within rock fractures induced by mineral dissolution under stress and temperature controlled conditions. Izadi and Elsworth (2015) studied the THMC processes in a discrete fracture network in a geothermal reservoir. They showed that the thermal stress and pore pressure effects are most prominent in inducing seismic events and triggering slip in early days of injection. In a later period of heat extraction, smaller seismic events were formed within the reservoir due to thermal and chemical effects. Further, Kamid et al. (2018) designed a geothermal power plant for simultaneous generation of thermal energy and the electric power, and evaluated the cost of drilling a well, as well as designing and construction of geothermal power plant. The estimated payback time is calculated as 15 years. Although substantial efforts have been made on the numerical modeling of multi-field coupling processes in reservoirs, there is still a challenge to accurately estimate the influence degree of stress and chemical reaction on the heat extraction process in EGS (Chen et al., 2018; Song et al., 2018; Yao et al., 2018; Wang et al., 2019).

The main objective of this study is to compare the influence of TH, THM and THMC coupling on heat production potential over a 30 year period in the deep hot dry rocks of the Songliao Basin, and analyze the interaction among thermal field, hydraulic field, mechanical field and chemical field. It is hoped to provide useful guidance for the practical exploitation of dry hot rock.

The novelty of this study mainly lies in two aspects. First, the establishment of the model is considered to be fully consistent with the actual geology, and the actual engineering geological data is adopted, making the research relatively practical. Second, the effects of TH, THM and THMC coupling on reservoir evolution characteristics have been compared in detail.

## 2. Program introduction and validation

### 2.1 Simulation program introduction

TOUGH2-EGS is a numerical simulation program coupling geomechanics and chemical reactions for fluid and heat flows in porous media and fractured reservoirs of enhanced geothermal systems. The simulator includes THM, THC and THMC simulations. In EGS or HDR, greater temperature gradient existing between rocks and circulating fluids, and the Multiple Interacting Continua (MINC) method used to treat the fracture medium can continuously subdivide the rock matrix, well simulating pressure and temperature transfer between the rock and the injected fluid. The program is developed from the linear elastic theory for the thermo-poro-elastic system and is formulated with the mean normal stress as well as pore pressure and temperature. The chemical reaction is sequentially coupled after solution of flow equations, which provides the flow velocity and phase saturation for the solute transport calculation at each time step. In addition, reservoir rock properties, such as porosity and permeability, are subjected to change due to rock deformation and chemical reactions (Hu et al., 2013). At present, TOUGH2-EGS has been widely used in geothermal reservoir engineering, nuclear waste and $CO_2$ geological disposal, environmental assessment and other fields (Fakcharoenphol et al., 2013; Huang et al., 2016; Yu et al., 2018).

### 2.2 Establishment of multi -field coupling numerical model

#### 2.2.1 The governing equation

For the phenomenon of heat and mass transfer of multiphase and multicomponent fluid in geothermal reservoir, the mathematical models established include the general governing equation, geomechanical equation and geochemical equation. The general governing equation of micro-unit is:

$$\frac{d}{dt}\int_{V_n}\mathbf{M}^k dV_n = \int_{\Gamma_n}\mathbf{F}^k\cdot\mathbf{n}d\Gamma_n + \int_{V_n}q^k dV_n \tag{1}$$

where $k$ = 1, ..., NK represents the component number; $n$ = 1,

..., NEL represents the grid number; $V_n$ is the volume of the calculated micro-unit, whose geometric boundary is $\Gamma_n$; vector $M$ is mass or energy per unit volume; vector $F$ is mass flow or heat flow; $q$ is the source/sink; $n$ is the normal vector of $d\Gamma_n$ on the surface of the micro-unit, pointing to the inside of micro-unit is positive.

In the mass balance equation, the left unsteady term is usually:

$$M^k = \sum \phi S_\beta \rho_\beta X_\beta^k \tag{2}$$

where $\beta$ = 1, ..., NPH is the phase number of the component; $\phi$ is the effective porosity; $\rho_\beta$ is the density of $\beta$ phase; $S_\beta$ is the phase saturation of $\beta$ phase; $X_\beta^k$ is the mass fraction of the $k$ component in $\beta$ phase.

For the calculation of mass flow, the liquid and gas phase flows are involved in the reservoir, which is described by the multi-phase Darcy law as follows:

$$\begin{aligned} F_\beta &= -k_0 \left(1 + \frac{b}{P_\beta}\right) \frac{k_{r\beta}\rho_\beta}{\mu_\beta} \left(\nabla P_\beta - \rho_\beta g\right) \\ \beta &= 1, \ldots, NPH \end{aligned} \tag{3}$$

where $k_0$ is the absolute permeability; $b$ is the gas slippage factor, $b$ = 0 when $\beta$ is liquid phase; $k_{r\beta}$ is the relative permeability of $\beta$ phase; $\mu_\beta$ is the dynamic viscosity; $P_\beta$ is the $\beta$ phase pressure; $g$ is gravity acceleration vector.

In the energy balance equation, the left unsteady term of Eq. (1) is:

$$M^k = (1-\phi)\rho_R C_R T + \phi \sum_\beta S_\beta \rho_\beta u_\beta \tag{4}$$

where $\rho_R$ and $C_R$ are the density and specific heat of host rock respectively; $T$ represents the temperature; $u_\beta$ represents the internal energy of $\beta$ phase.

The calculation of the heat flow needs to consider heat conduction, heat convection and radiation heat transfer. The expression is:

$$\begin{aligned} F^k = &-\left[(1-\phi)\lambda_R + \phi \sum_{\beta=1,2,3} S_\beta \lambda_\beta\right] \nabla T \\ &+ f_\sigma \sigma_0 \nabla T^4 + \sum_{\beta=1,2} h_\beta F_\beta \end{aligned} \tag{5}$$

where $\lambda$ is the thermal conductivity; $h_\beta$ is the specific enthalpy of $\beta$ phase; $f_\sigma$ is the surface radiation factor; $\sigma_0$ is the Boltzmann constant.

This method assumes that the boundaries of each micro-unit can be deformed as an elastic material and obey the generalized Hooke's law. The geomechanical governing equation can be expressed as:

$$M = 0 \tag{6}$$

$$\begin{aligned} &\frac{3(1-v)}{(1+v)} \nabla^2 \sigma_m + \nabla \cdot \bar{F} \\ &- \frac{2(1-2v)}{(1+v)} \left(\alpha \nabla^2 P + 3\beta K \nabla^2 T\right) = 0 \end{aligned} \tag{7}$$

For multi-porosity media with the MINC method, the geomechanical governing equations is:

$$\begin{aligned} &\frac{3(1-v)}{(1+v)} \nabla^2 \sigma_m + \nabla \cdot \bar{F} - \sum_j \frac{2(1-2v)}{(1+v)} \\ &\left(\alpha_j \nabla^2 P_j + 3\beta_j K_j \nabla^2 T_j\right) = 0 \end{aligned} \tag{8}$$

where $\alpha$ is the Biot's coefficient; $\beta$ is the linear thermal expansion coefficient; $K$ is the bulk modulus; $\sigma_m$ is the mean normal stress; $\bar{F}$ is the body force; $v$ is the Poisson's ratio.

The governing equation for geochemical reactions is:

$$M^k = \phi S_k C_{kl} \tag{9}$$

$$\begin{aligned} F^k &= v_l C_{kl} - (\tau \phi S_l D_l) \nabla C_{kl} \\ k &= 1, \ldots, N_l \end{aligned} \tag{10}$$

where $N_l$ is the total number of chemical components in the liquid phase; $C_{kl}$ is the concentration of the $k^{th}$ species in the liquid phase; $v_l$ is the Darcy velocity; $D_l$ is the diffusion coefficient.

Mineral saturation is used to determine the dissolution and precipitation of minerals. When the saturation is positive, it indicates mineral precipitation; the saturation is negative, it indicates mineral dissolution; the saturation is zero, it indicates that it is in equilibrium. The mineral saturation ratio can be expressed as:

$$\begin{aligned} \Omega_m &= X_m^{-1} \lambda_m^{-1} K_m^{-1} \prod_{j=1}^{N_c} c_j^{\nu_{mj}} \gamma_j^{\nu_{mj}} \\ m &= 1, \ldots, N_p \end{aligned} \tag{11}$$

where $m$ is the mineral index; $X_m$ is the mineral mole fraction of the $m^{th}$ phase; $\lambda_m$ is its thermodynamic activity coefficient; $K_m$ is the equilibrium constant.

### 2.2.2 Hydraulic properties correlations

For fracture network, Rutqvist et al. (2002) defined the aperture width $b_i$ in the $i$ direction as function of effective stress:

$$b_i = b_{0,i} + \Delta b_i = b_i + b_{\max}\left(e^{-d\sigma'} - e^{-d\sigma_0'}\right) \tag{12}$$

The correlation between the fracture porosity and the aperture width $b_i$ is:

$$\phi = \phi_0 \frac{b_1 + b_2 + b_3}{b_{1,0} + b_{2,0} + b_{3,0}} \tag{13}$$

The permeability in the $i$ direction is related to the aperture width in the $j$ and $k$ directions, and the correlation is:

$$k_i = k_{i,0} \frac{b_j^3 + b_k^3}{b_{j,0}^3 + b_{k,0}^3} \tag{14}$$

The porosity of the reservoir matrix and fracture is directly related to the volume of rock mineral, and the volume of

the rock mineral will change due to the dissolution and precipitation process. Therefore, the porosity calculation formula (matrix or fracture) is:

$$\phi = 1 - \sum_{m=1}^{N_m} fr^m - fr^u \tag{15}$$

where $N_m$ is the number of reactive minerals; $fr^m$ is the volume fraction of reactive minerals in rocks ($V_{mineral}$ / $V_{medium}$); $fr^u$ is the volume fraction of non-reactive minerals in rocks.

The permeability change caused by chemical reactions is different for reservoir matrix and fracture. In the matrix, the correlation between permeability and porosity can be expressed by the Carman-Kozeny equation:

$$k = k_i \frac{(1-\phi_i)^2}{(1-\phi)^2} \left(\frac{\phi}{\phi_i}\right)^3 \tag{16}$$

In the fracture, based on the assumption of plane parallel fracture of uniform aperture, the modified permeability can be approximately calculated according to the change of porosity:

$$k = k_i \left(\frac{\phi}{\phi_i}\right)^3 \tag{17}$$

The disadvantage of the above correlation is that when the porosity is 0, the fracture permeability is also 0, which is inconsistent with the experimental results and the actual situation. Therefore, more accurate correlations based on fracture aperture have been proposed. The initial aperture is:

$$b_0 = (12 k_0 s)^{\frac{1}{3}} \tag{18}$$

where $k_0$ is the initial fracture permeability; $s$ is the fracture spacing.

The permeability change caused by the change in aperture is:

$$k = \frac{(b_0 + \Delta b)^3}{12s} \tag{19}$$

Xu et al. (2004) proposed the correlation between $\Delta b$ and porosity $\phi$:

$$\Delta b = \frac{(\phi - \phi_0)}{\phi_0} b_g \tag{20}$$

where $\Delta b$ is the aperture change caused by mineral dissolution and precipitation; $b_g$ is the geometric aperture, and its value is equal to the ratio of the initial porosity $\phi_0$ to the fracture surface area $A_f$.

The influence of geomechanics and geochemistry should be considered to the change of reservoir rock properties. Mathematically, the porosity change is calculated as the summation of geomechanical and geochemical induced changes:

$$\phi = \phi_0 + \Delta\phi_m + \Delta\phi_c \tag{21}$$

For rock matrix, the change of permeability can be calculated according to Eq. (16). For rock fracture, the change of permeability can be calculated from the change of aperture:

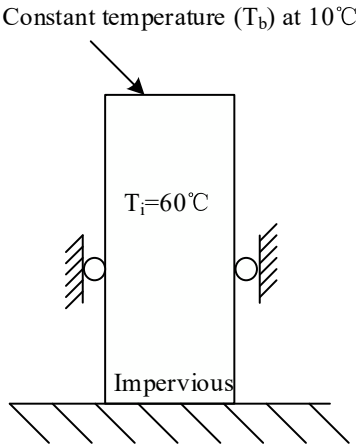


**Fig. 1.** Illustration of the 1-D heat conduction.

$$b = b_0 + \Delta b_m + \Delta b_c \tag{22}$$

where subscript 0 represents the initial state; subscripts $m$ and $c$ represent the changes caused by geomechanics and geochemistry respectively.

## 2.3 Program validation

The TOUGH2-EGS program use the integral finite difference method to discretize the mass and energy balance equations, and the accuracy has been tested by comparison with many different analytical and numerical solutions (Fakcharoenphol et al., 2013). The program will be shortly verified from three aspects as follows.

### 2.3.1 1-D heat conduction

The 1-D heat conduction problem is a non-permeable column that undergoes uniaxial strain in the vertical direction only. The column is subjected to a constant temperature on the top. Only heat conduction takes place. A non-permeable solid column with very small porosity was initialized with the temperature of 60 °C. A low temperature of 10 °C was imposed at the top column. Fig. 1 illustrates the problem of the 1-D heat conduction under constant surface temperature. Bai (2005) deduced the analytical solution of the 1-D heat conduction problem by finite Fourier transform and its inverse transform. The comparison result is plotted in Fig. 2, which respectively show the temperature and displacement evolution at different time in the solid column. The results of the analytical model by Bai (2005) are also presented for comparison. It can be observed that the numerical results agree well with the analytical model, this verifies the accuracy of the TOUGH2-EGS program.

### 2.3.2 2-D compaction

Next, this paper considers the 2-D compaction problem, which is depicted as Fig. 3. A constant compressive force is applied to the top of a fluid-filled poroelastic material, inducing an instantaneous uniform pore pressure increase and

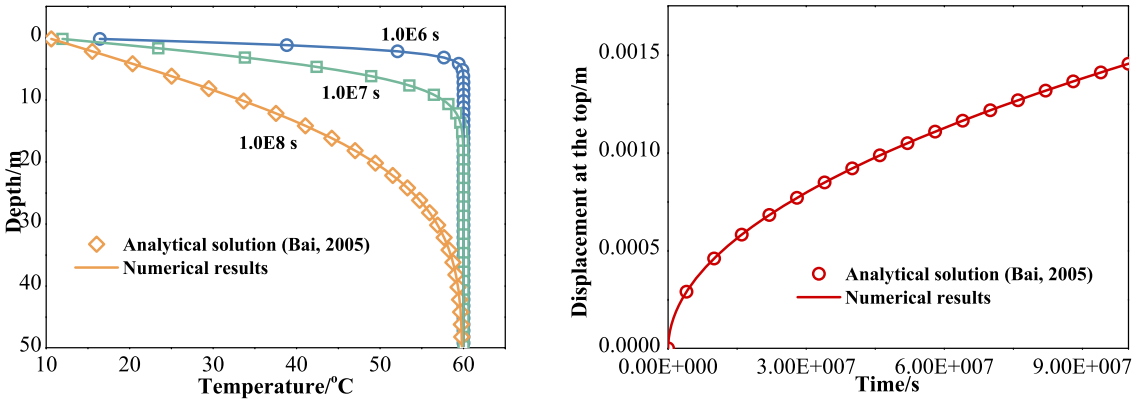


(a) Temperature profiles

(b) Displacement of the top column

**Fig. 2.** Comparison between numerical results and analytical solutions.

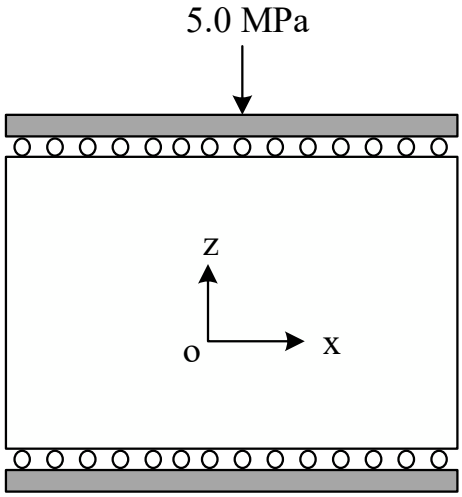


**Fig. 3.** Schematic of 2-D compaction.

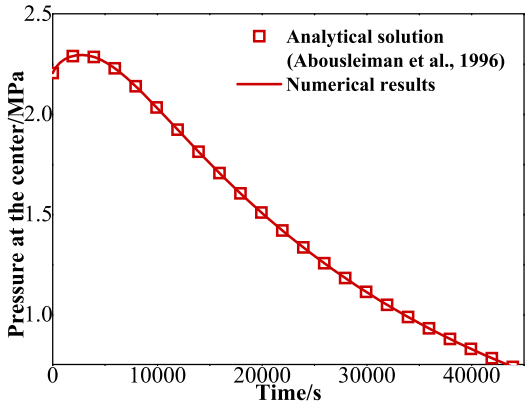


**Fig. 4.** Pore pressure profile at the center of domain.

compression. Afterwards, the material is allowed to drain laterally. The pore pressure near the edges will decrease due to drainage, the material there becomes less stiff and there is a load transfer to the center, resulting in a further increase in center pore pressure that reaches a maximum and then declines. Abousleiman et al. (1996) presented an analytical solution to this problem.

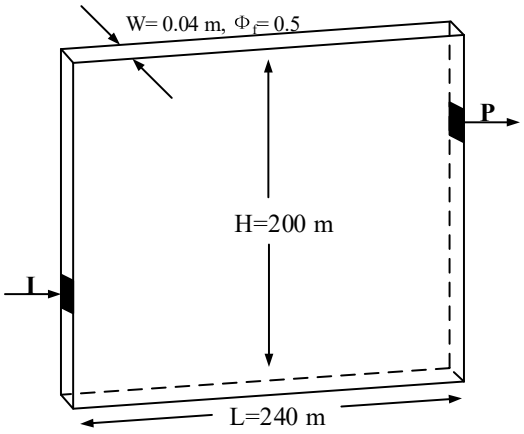


**Fig. 5.** Schematic diagram of the model in vertical fracture injection occurs at I, production at P.

The initial pore pressure and mean stress were 0.1 MPa. Then, the addition stress of 5.0 MPa was imposed and produced the pore pressure increase. When the system to reach equilibrium, it was allowed to drain from both sides with the pressure of 0.1 MPa. Fig. 4 shows the comparison of pressure at the center of the domain between the numerical and the analytical solution. The numerical result has a peak and shows excellent agreement with the analytical solution, which lends creditability to our computational approach again.

### *2.3.3 Heat sweep in a vertical fracture*

The fracture is bounded by semi-infinite half-spaces of impermeable rock, which provide a conductive heat supply. Initial temperature is 300 °C throughout. Water at 100 °C temperature is injected at one side of the fracture at a constant rate of 3.75 kg/s, while production occurs at the other side

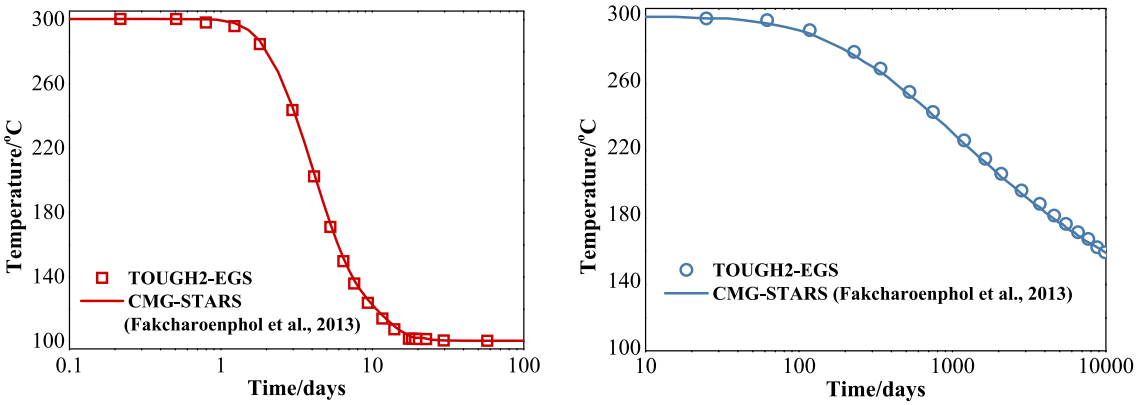


(a) No heat gain from surrounding rock (b) Heat gain from surrounding rock

**Fig. 6.** Comparison of the simulated production temperature between CMG-STARS and TOUGH2-EGS results.

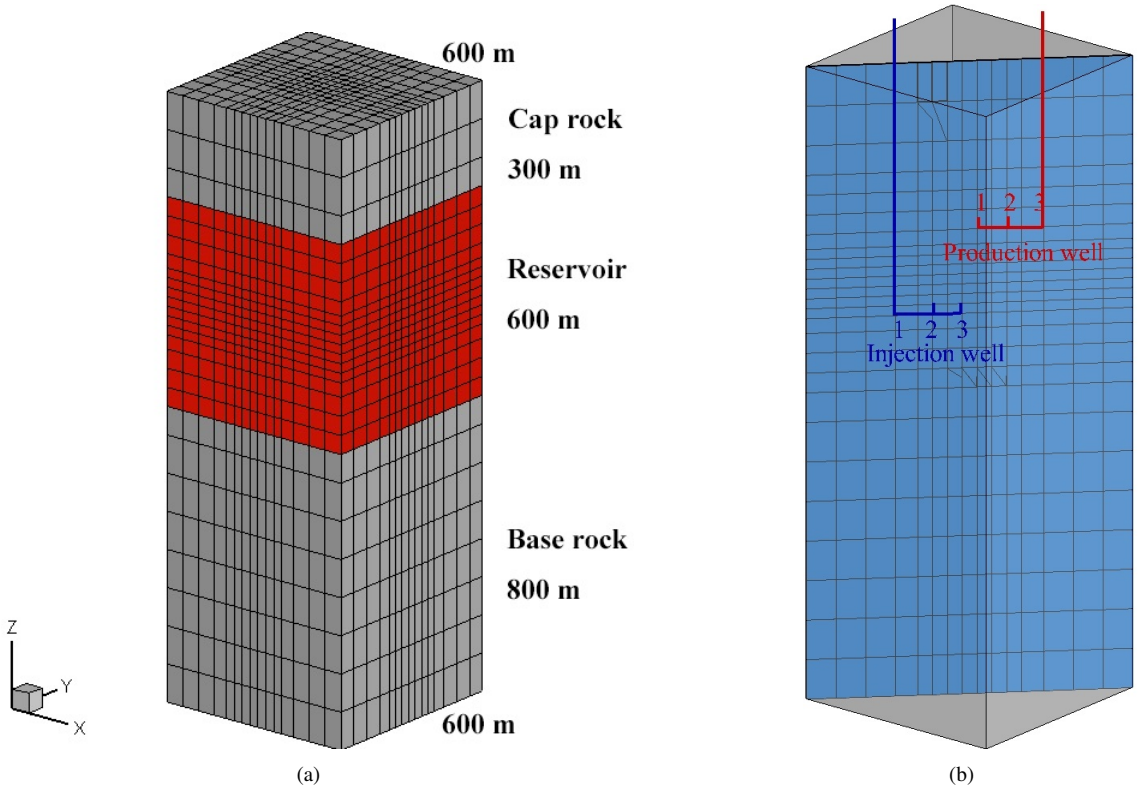


(a) (b)

**Fig. 7.** Schematic of the reservoir model and well arrangement.

against a specified wellbore pressure, as illustrated in Fig. 5.

Two cases were run to demonstrate the accuracy of the TOUGH2-EGS program. Fakcharoenphol et al. (2013) used a non-isothermal commercial reservoir simulator of computer modeling group (CMG-STARS) to study this problem with high reliability, and this paper compares the simulation results with the CMG-STARS results. Fig. 6(a) shows the production temperature comparison without obtaining heat from surrounding rock between CMG-STARS and TOUGH2-EGS. Numerical results of the production temperature of heat gain from surrounding rock is presented in Fig. 6(b). It can be found that the results of TOUGH2-EGS are very close to those of the CMG-STARS.

## 3. Numerical model and boundary conditions

### *3.1 Model establishment*

The Songliao Basin is located in the northeastern part of China and is a high heat flow area in nationwide scope. It spans Heilongjiang, Jilin, Liaoning provinces and Inner Mongolia Autonomous Region. In this paper, 3,500 to 5,200 m with high degree of fracture growth in Songliao Basin is selected as the research object. A numerical model based on MINC method is

established to analyze the evolution of reservoir temperature, porosity-permeability property and chemical fields among TH, THM and THMC coupling. The established model diagram and injection-production well distribution are shown in Fig. 7.

The model mesh uses the multi-grid subdivision method of TOUGH2-EGS. In the main grid, the width of every gridblock between the injection-production well is 25 m, the width of every gridblock outside of this region is 50 m, and the height of every gridblock in the cap rock and the base rock is 100 m. In the $x$ direction or $y$ direction, the simulated domain is divided into 16 gridblocks. In the $z$ direction, this is divided into 27 gridblocks. The total number of main grids is 6,912. On the basis of the main meshing, the reservoir domain is divided into three continua, the first continuum represents the fracture network and its volume fraction is 0.01; the other two continua represent the rock matrix, and their volume fraction is 0.34 and 0.65. After this partition, there are a total of 15,104 subgrid blocks nested in the 6,912 gridblocks.

### 3.2 Parameters and boundary conditions

Combined with the actual engineering geological data of the northern part of the Songliao Basin and the field monitoring results of the Yingshen well regions (Guo et al., 2016), the main computational parameters used in this simulation are listed in Table 1.

The lithology of the simulated thermal reservoirs is mainly rhyolite. The mineral composition of the rocks used in the chemical reaction coupling is shown in Table 2. The chemical composition of the reservoir water is listed in Table 3 (Bao et al., 2014).

The effect of the temperature gradient is considered in this simulation. The top depth of the model is 3,500 m and the initial reservoir temperature is 150 °C; the bottom depth is 5,200 m and the temperature is 201 °C. The corresponding initial reservoir pressure is gradually increased from 36 to 53 MPa. For the boundary at the top, this paper neglects the slight conductive heat exchange between the permeable reservoir and the impermeable cap rock, the reservoir are set as no-flow for mass and heat. For the boundary at the bottom, the reservoir are set as no-flow for mass, the temperature is set to a constant value. Because of symmetry, lateral boundaries of the reservoir are also no-flow for mass and heat. The injection water temperature is about 25 °C and the performance of fractured reservoir for a period of 30 years has been investigated.

## 4. Results and analysis

The injection of low temperature water during EGS operation process will inevitably cause changes in temperature field, porosity-permeability property and chemical field in the thermal reservoir. The effects of TH, THM and THMC coupling on reservoir evolution characteristics have been compared in detail below.

### 4.1 Evolution of temperature field

The coupling of thermal, hydraulic, mechanical and chemical has an important influence on the numerical simulation of heat extraction in geothermal reservoirs. In order to further evaluate their effects on the EGS outlet temperature, the evolution of the production temperature against different simulation time is illustrated in Fig. 8. It can be found that compared with the TH coupling, the effect of the THM and THMC coupling on the production temperature is sensitive. A stable running condition for about 5 years with no significant difference can be observed for all these three cases. During the period of 5 to 30 years, the low-temperature zone expands gradually to the

**Table 1.** Reservoir physical parameters.

| Parameter | Value | Parameter | Value |
|---|---|---|---|
| Youngs module (GPa) | 14.4 | Rock matrix porosity | 0.05 |
| Poisson ratio | 0.2 | Rock matrix permeability ($m^2$) | $3.2 \times 10^{-16}$ |
| Biot's coefficient | 1 | Fracture porosity | 0.1 |
| Linear thermal expansion ($°C^{-1}$) | $4.14 \times 10^{-6}$ | Fracture permeability ($m^2$) | $3.2 \times 10^{-14}$ |
| Rock specific heat (J/kg°C) | 1,000 | Productivity index | $1.03 \times 10^{-12}$ |
| Rock density ($kg/m^3$) | 2,600 | Water injection rate (kg/s) | 8 |
| Rock thermal conductivity (W/m·°C) | 2 | Bottomhole production pressure (MPa) | 33.25 |

**Table 2.** Initial volume fraction of reactive minerals.

| Mineral | Volume fraction | Mineral | Volume fraction |
|---|---|---|---|
| Quartz | 0.39 | Anorthite | 0.02 |
| Muscovite | 0.16 | Illite | 0.05 |
| Albite | 0.18 | Clinochlore | 0.08 |
| Calcite | 0.03 | Clinozoisite | 0.01 |

**Table 3.** Fluid chemical compositions used in simulations.

| Chemical component | $HCO_3^-$ | $Cl^-$ | $Ca^{2+}$ | SiO2(aq) | $K^+$ | $Na^+$ | $AlO_2^-$ |
|---|---|---|---|---|---|---|---|
| Reservoir fluid (mmol/L) | 0.53 | 220 | 0.53 | 2.68 | 7.18 | 212.8 | 0.006 |
| Injection fluid (mmol/L) | 0.53 | 220 | 0.16 | 2.58 | 7.18 | 210.9 | 0.002 |

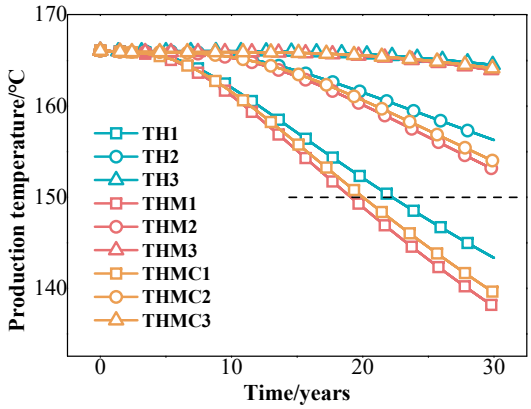


**Fig. 8.** Production temperature curves during 30 years period.

production well and the heat production of the system decreases. At the production well 1 in 30 years, the production temperature of the TH, THM and THMC coupling is approximately 86%, 83% and 84% of the reservoirs initial temperature, respectively. However, Garnish et al. insisted that temperature drop during the entire production life should be less than 10% (Baria et al., 1999), and compared with TH and THMC coupling, the service-life for THM coupling decreased by 1,140 days and 332 days, respectively. It seemed that the consideration of mechanical field and chemical field is much more significant to the production temperature in reservoir simulation.

The temperature contour in Fig. 9 suggests that the area around the injection point is cooled initially, and an expanding elliptical area of the cooled region is formed. The downward flow is held back at the boundary of the base rock, forming the border of the cooled region. Meanwhile, the temperature around the production well has no significant change. After 10 years of operation, the cooling zone expands to the production well 1, but the difference of temperature field is very small among the three cases. The reason is that the running time is relatively short, and the effect of mechanical field and chemical field on reservoir temperature evolution is limited, which can also be envisaged from the production temperature curves in Fig. 8. As time passes, the difference will emerge gradually. Fig. 9(b) shows the comparison of simulation results at the injection-production well plane among TH, THM and THMC coupling after 30 years fluid injection. It can be seen from these three figures that the cold front of the low temperature region of the THM coupling expands slightly faster than TH and THMC coupling, the production temperature near the production well 1 is also getting lower.

The comparison of temperature field in the reservoir with and without the presence of the mechanical field and the chemical field after 30 years is plotted in Fig. 10. When the mechanical field exists, the area of the cooled region is relatively large, and considering both the mechanical field and the chemical field, the low temperature area moves faster than TH coupling, but slower than THM coupling. As a result of analysis, the mechanical and chemical field play a vital role in reservoir heat extraction.

## 4.2 Evolution of porosity-permeability property

The TH coupling has no effect on porosity and permeability parameters, so there is no change in porosity and per-

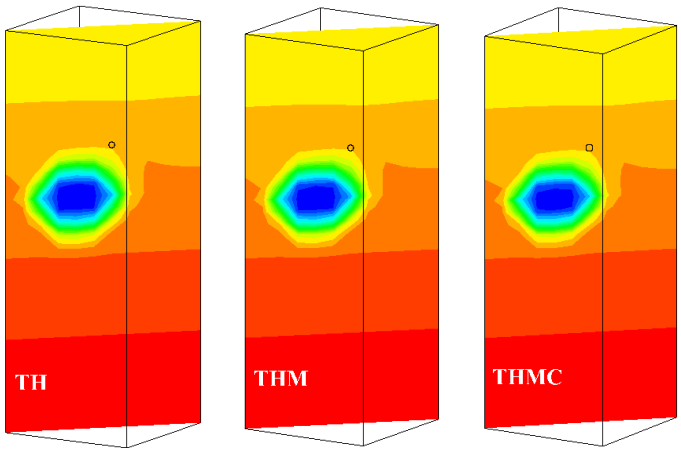


(a) 10 years

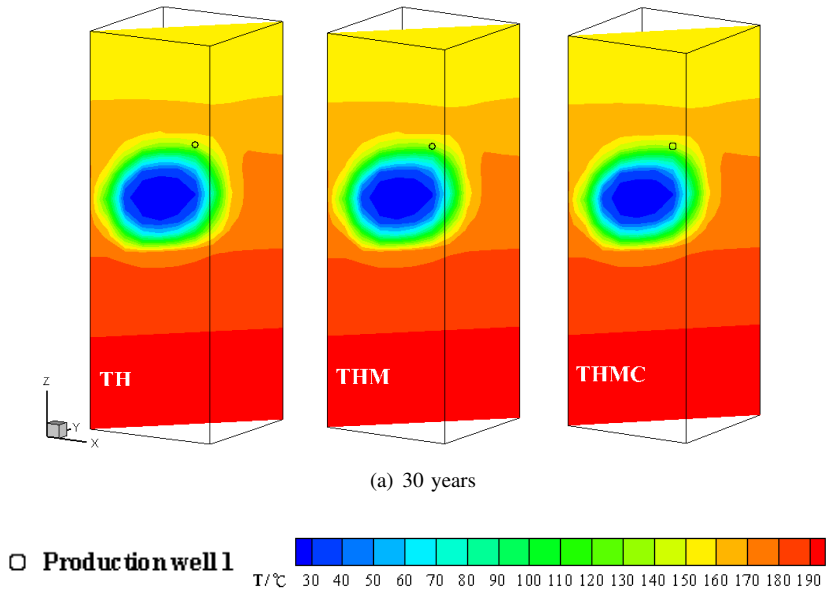


(a) 30 years

**Fig. 9.** Comparison of the temperature field at the injection-production well plane.

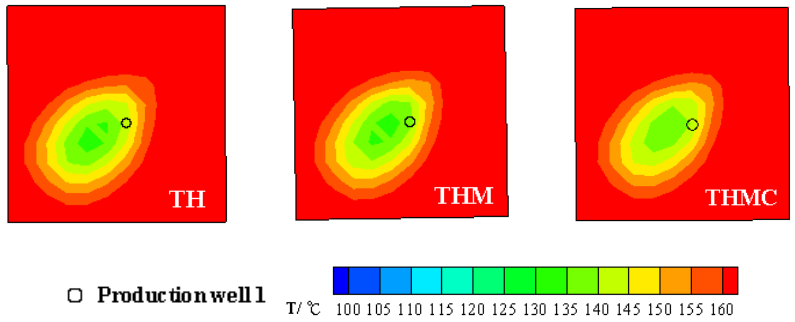


**Fig. 10.** Comparison of temperature field at the horizontal section of production well after 30 years.

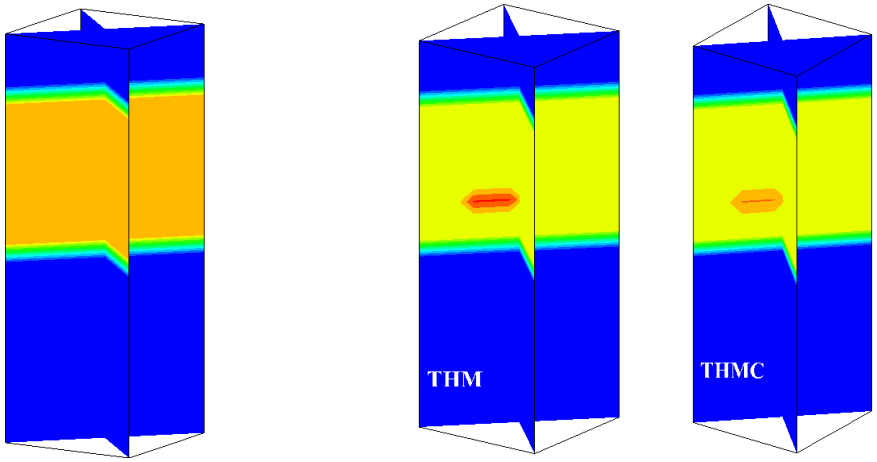


(a) 0 year (b) 1 year

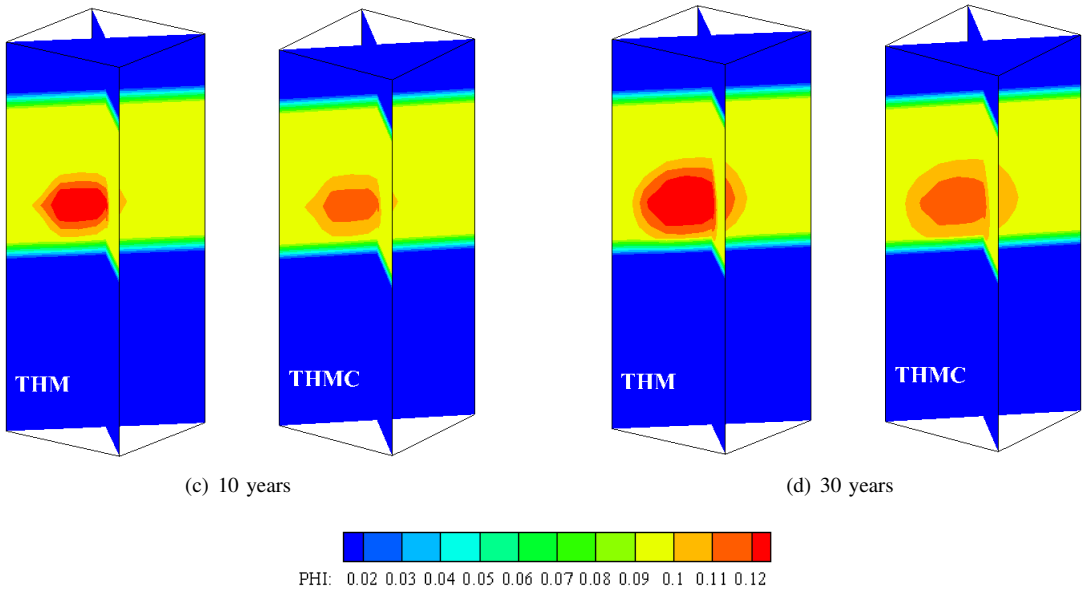


(c) 10 years (d) 30 years

**Fig. 11.** Comparison of the porosity evolution.

meability of reservoir fractures during the 30-year simulation period, as shown in Figs. 11(a) and 12(a). For the THM and THMC coupling, the porosity and permeability parameters near the injection point first increase, and as the simulation time continues, it continues to extend from the injection point to the surrounding area. Finally, the porosity and permeability in most area of the fractured zone is increased. Figs. 11 and 12 show the porosity and permeability variation over production. It can be seen that the maximum porosity and permeability in the THMC coupling simulation run is lower than THM coupling run, it is because the mechanical enhanced effects are offset by the chemical precipitation.

For a more detailed description of the variation of the porosity and permeability parameters, the evolution of the maximum porosity and permeability with time is shown in Fig. 13. The cooling effect of injection induces a decrease of the thermal stress, causing contraction of the rock matrix, simultaneously raises the porosity and permeability. Meanwhile, due to water injection, pore pressure changes and alters the porosity and permeability. At the initial stage of thermal exploitation, the porosity and permeability of THM and THMC coupling increase rapidly. Porosity of injection point increases from initial 0.1 to 0.13 and 0.115 respectively, and permeability of injection point increases from $3.2 \times 10^{-14}$ to $7.52 \times 10^{-14}$ and $5.04 \times 10^{-14}$ respectively. At approximately the end of production, the porosity and permeability of THMC coupling are about 88% and 67% of those of THM coupling.

Reservoir volume with altered porosity and permeability increases approximately linearly, as shown in Fig. 14. The reservoir volume increase of THM coupling is greater than that of THMC coupling, which is consistent with the cloud picture distribution in Fig. 12. Meanwhile, the variation trend

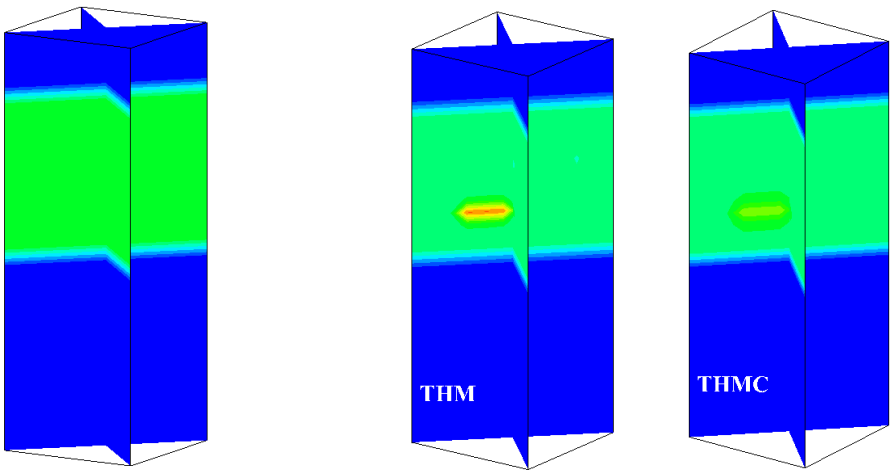


(a) 0 year (b) 1 year

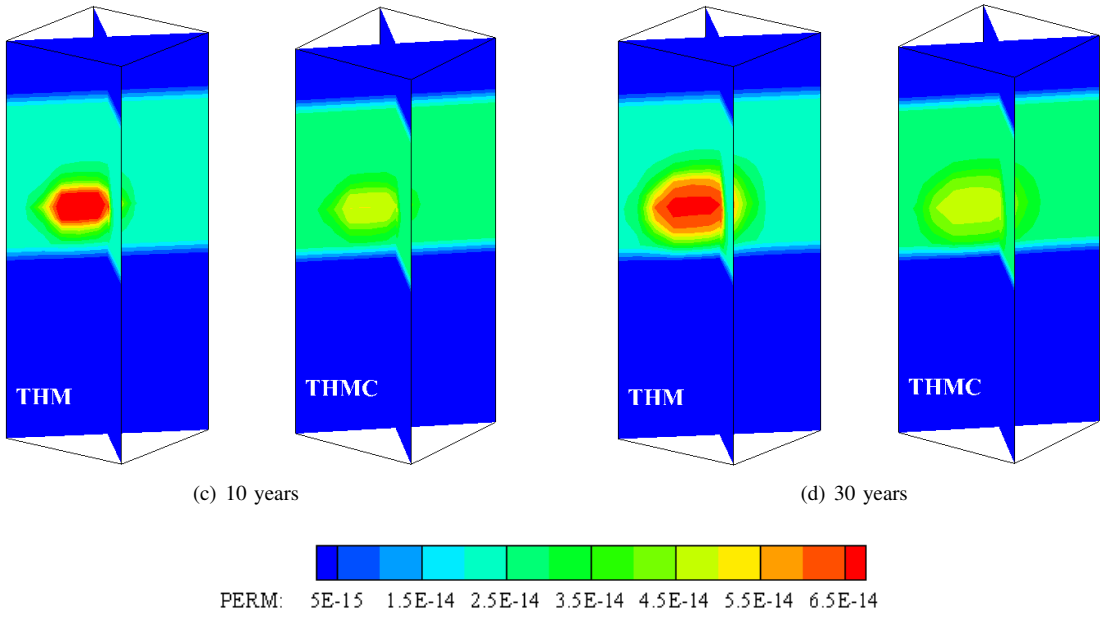


(c) 10 years (d) 30 years

**Fig. 12.** Comparison of the permeability evolution.

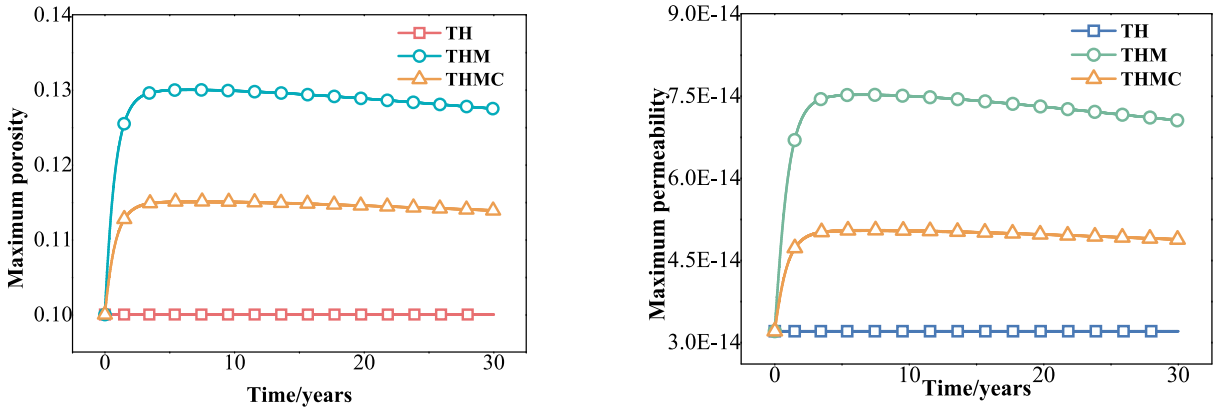


(a) Maximum porosity (b) Maximum permeability

**Fig. 13.** Evolution of maximum porosity and permeability with time.

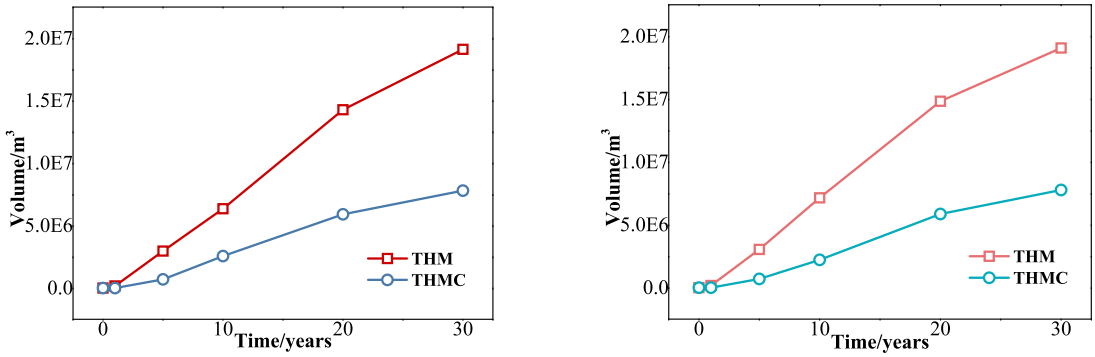


(a) Porosity change more than 10% (b) Permeability change more than 30%

**Fig. 14.** Evolution of reservoir volume with changes in porosity and permeability.

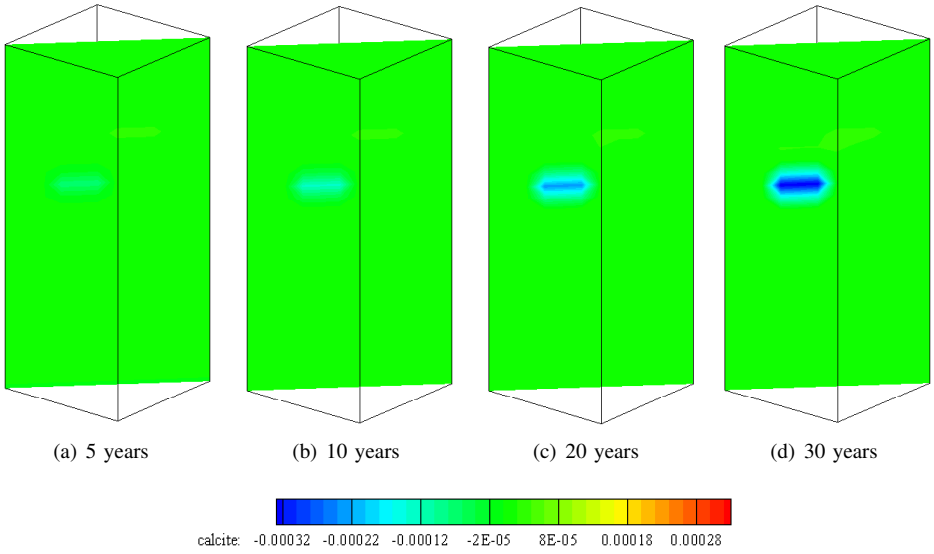


**Fig. 15.** Evolution of calcite volume fraction with time

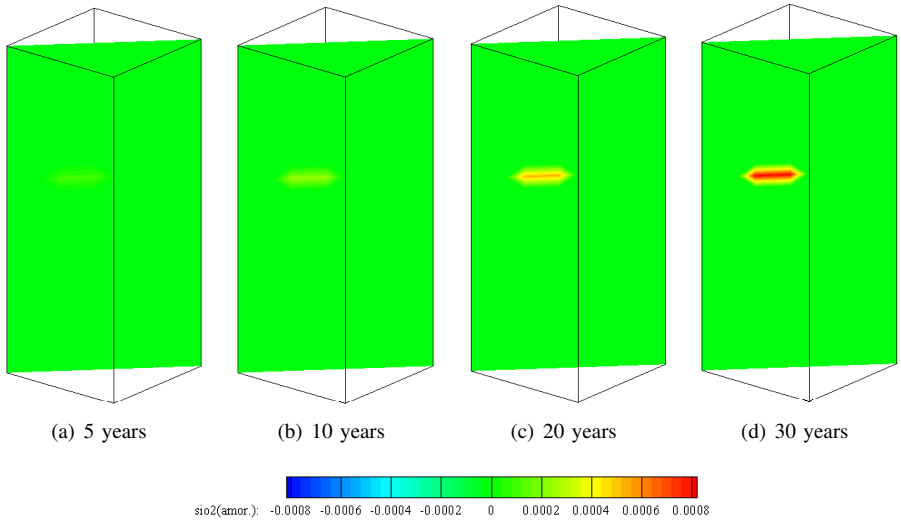


**Fig. 16.** Evolution of amorphous $SiO_2$ volume fraction with time.

of reservoir volume with porosity change more than 10% and permeability change more than 30% is similar, which is consistent with Eq. (17). After thirty years injection, the changed reservoir volume in the coupling of THM and THMC accounts for about 8.8% and 3.6% of the total fracture zone, respectively.

## 4.3 Evolution of chemical field

In a real scenario, chemical reactions are also involved in the THMC coupling process, and clear dissolution / precipitation and distribution of mineral in the fractured zone have an important impact on geothermal heat extraction. The negative values in Figs. 15 and 16 correspond to dissolution and the positive values correspond to precipitation.

The solubility of calcite increases with the decrease of

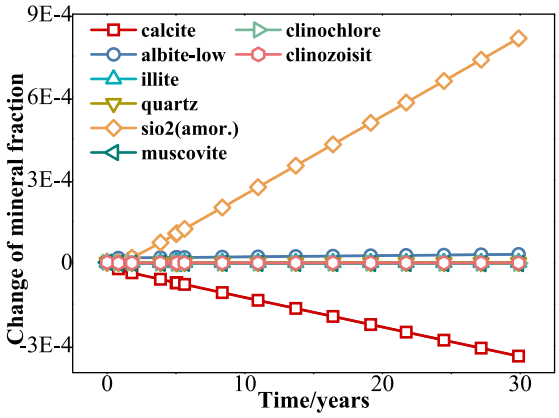


**Fig. 17.** Volume fraction change of mineral around injection well.

temperature. As shown in Fig. 15, the calcite gradually dissolves near the injection well due to the injection of low temperature water. Meanwhile, the dissolved amount of calcite increases with the increase of simulated time. In the 30 years, the volume fraction of calcite near the injection well decreased by 0.034%.

The volume fraction change of amorphous $SiO_2$ with time is shown in Fig. 16. It can been seen that the chemical precipitation concentrates around the injection well and only reaches 34 meters after 30 years injection. The closer to the injector, the higher precipitation effects is observed. In the simulation period of 30 years, the volume fraction of amorphous $SiO_2$ increases by 0.08%.

The change of abundance of minerals affects the reservoir performance by changing the porosity and permeability. The change of abundance of minerals is due to the chemical reaction among the species and rock minerals. The Fig. 17 shows the $SiO_2$ (Amorphous) has the largest positive value, which means it is the most precipitated minerals, and calcite has the smallest negative values, which means calcite the most dissolved minerals. But the precipitation from $SiO_2$ is much larger than dissolution of calcite, which explains the porosity and permeability decrease in Figs. 11 and 12. The albite also has a small amount of precipitation, but the dissolution and precipitation reactions of other minerals are negligible because the variation is almost zero.

## 5. Conclusions

This paper presents numerical simulation considering individual (TH, THM) and combined THMC effects during cold water injection to study the evolution characteristics of temperature field, porosity-permeability property and chemical field in EGS reservoir. Based on the study results, the following conclusions are made.

1) The stable production stage of the three cases is approximately 5 years, as the heat production goes on, the outlet temperature continually decreases. Compared with TH and THMC coupling, the service-life for THM coupling decreased by 1,140 days and 332 days, respectively. When considering both the mechanical field and the chemical field, the low temperature area moves faster than TH coupling, but slower than THM coupling.
2) Considering the influence of temperature, stress and chemical reaction, the porosity and permeability of the whole fracture area are elevated. The porosity and permeability of THMC coupling are about 88% and 67% of those of THM coupling, and the changed reservoir volume with porosity change more than 10% and permeability change more than 30% accounts for about 3.6% and 8.8% of the total fracture zone, respectively.
3) Calcite is the most dissolved mineral with volume fraction reduced by 0.034%, and the precipitation of $SiO_2$ (Amorphous) is the largest, the volume fraction increases by 0.08%. During the entire production life, the precipitation from $SiO_2$ is much larger than dissolution of calcite.

In this study, based on the geological data of Songliao basin, the practical model has been developed for simulating the actual EGS heat extraction process, and the effects of TH, THM and THMC coupling on reservoir properties were compared. This results should be helpful for the development of HDR geothermal energy.

## Nomenclature

### *Abbreviations*

$A_f$ = fracture surface area
$b$ = gas slippage factor
$b_g$ = geometric aperture
$\Delta b$ = aperture change
$C$ = specific heat
$D$ = diffusion coefficient
$F$ = mass flow or heat flow
$\bar{F}$ = body force
$f_\sigma$ = surface radiation factor
$fr$ = volume fraction
$g$ = gravity acceleration
$h$ = specific enthalpy
$k$ = permeability
$K$ = bulk modulus
$K_m$ = equilibrium constant
$m$ = mineral index
$M$ = mass or energy
$P$ = pressure
$q$ = source / sink
$s$ = fracture spacing
$S$ = phase saturation
$T$ = temperature
$u$ = internal energy
$X$ = mass fraction
$V_n$ = volume

### *Greek symbols*

$\Gamma_n$ = geometric boundary
$\alpha$ = Biot's coefficient
$\beta$ = Linear thermal expansion coefficient
$\phi$ = porosity
$\lambda$ = thermal conductivity
$\lambda_m$ = thermodynamic activity coefficient
$\mu$ = viscosity
$v$ = Poisson's ratio
$v_l$ = Darcy velocity
$\rho$ = density
$\sigma_0$ = Boltzmann constant
$\sigma_m$ = mean normal stress

## Acknowledgments

The authors gratefully appreciate the financial support from the Project of the National Natural Science Foundation of China (No. 51936001), the Fundamental Research Funds of Central Universities (No.18CX07012A and No.19CX05002A).

## References


Abousleiman, Y., Cheng, A.H.D., Cui, L., et al. Mandels problem revisited. Geotechnique 1996, 46(2): 187-195.

Bai, B. One-dimensional thermal consolidation characteristics of geotechnical media under non-isothermal condition. Eng. Mech. 2005, 22(5): 186-191.

Bao, X., Wu, Y., Wei, M., et al. Impact of water/$CO_2$-rock interactions on formation physical properties in EGS. Sci. Technol. Rev. 2014, 32(14): 42-47.

Baria, R., Baumgartner, J., Rummel, F., et al. HDR/HWR reservoir: Concepts, understanding and creation. Geothermics 1999, 28(4-5): 533-552.

Chen, T., Liu, G., Liao, S. A comparison study of reservoir boundary conditions of Enhanced Geothermal Systems (EGS). Energy Procedia 2019, 160: 301-309.

Chen, Y., Ma, G., Wang, H. The simulation of thermo-hydro-chemical coupled heat extraction process in fractured geothermal reservoir. Appl. Therm. Eng. 2018, 143: 859-870.

China Geological Survey. China geothermal energy development report. 2018-08-25.

Fakcharoenphol, P., Xiong, Y., Hu, L., et al. User's Guide of TOUGH2-EGS. A Coupled Geomechanical and Reactive Geochemical Simulator for Fluid and Heat Flow in Enhanced Geothermal Systems Version 1.0. Colorado School of Mines, Golden, CO (United States), 2013.

Guo, L., Zhang, Y., Yu, Z., et al. Hot dry rock geothermal potential of the Xujiaweizi area in Songliao Basin, northeastern China. Environ. Earth Sci. 2016, 75(6): 470.

Han, S., Cheng, Y., Gao, Q., et al. Investigation on heat extraction characteristics in randomly fractured geothermal reservoirs considering thermos-poroelastic effects. Energy Sci. Eng. 2019, 7: 1705-1726.

Huang, X., Zhu, J., Li, J., et al. Parametric study of an enhanced geothermal system based on thermo-hydro-mechanical modeling of a prospective site in Songliao Basin. Appl. Therm. Eng. 2016, 105: 1-7.

Huang, Z., Winterfeld, P.H., Xiong, Y., et al. Parallel simulation of fully-coupled thermal-hydro-mechanical processes in $CO_2$ leakage through fluid-driven fracture zones. Int. J. Greenhouse Gas Control 2015, 34: 39-51.

Hu, L., Winterfeld, P.H., Fakcharoenphol, P., et al. A novel fully-coupled flow and geomechanics model in enhanced geothermal reservoirs. J. Pet. Sci. Eng. 2013, 107: 1-11.

Ijeje, J.J., Gan, Q., Cai, J. Influence of permeability anisotropy on heat transfer and permeability evolution in geothermal reservoir. Adv. Geo-Energy Res. 2019, 3(1): 43-51.

Izadi, G., Elsworth, D. The influence of thermal-hydraulic-mechanical-and chemical effects on the evolution of permeability, seismicity and heat production in geothermal reservoirs. Geothermics 2015, 53: 385-395.

Kazemi, H., Ehyaei, M.A. Energy, exergy, and economic analysis of a geothermal power plant. Adv. Geo-Energy Res. 2018, 2(2): 190-209.

Liu, G., Zhou, B., Liao, S. Inverting methods for thermal reservoir evaluation of enhanced geothermal system. Renewable Sustainable Energy Rev. 2018, 82: 471-476.

Liu, X., Liu, Q., Liu, B., et al. Numerical manifold method for thermalhydraulic coupling in fractured enhance geothermal system. Eng. Anal. Bound. Elem. 2019, 101: 67-75.

Ogata, S., Yasuhara, H., Kinoshita, N., et al. Modeling of coupled thermal-hydraulic-mechanical-chemical processes for predicting the evolution in permeability and reactive transport behavior within single rock fractures. Int. J. Rock Mech. Min. Sci. 2018, 107: 271-281.

Rutqvist, J., Wu, Y., Tsang, C., et al. A modeling approach for analysis of coupled multiphase fluid flow, heat transfer, and deformation in fractured porous rock. Int. J. Rock Mech. Min. Sci. 2002, 39(4): 429-442.

Song, X., Shi, Y., Li, G., et al. Numerical simulation of heat extraction performance in enhanced geothermal system with multilateral wells. Appl. Energy 2018, 218: 325-337.

Sun, Z., Zhang, X., Xu, Y., et al. Numerical simulation of the heat extraction in EGS with thermal-hydraulic-mechanical coupling method based on discrete fractures model. Energy 2017, 120: 20-33.

Wang, Y., Li, T., Chen, Y., et al. A three-dimensional thermo-hydro-mechanical coupled model for enhanced geothermal systems (EGS) embedded with discrete fracture networks. Comput. Method. Appl. M 2019, 356: 465-489.

Wei, X., Feng, Z., Zhao, Y. Numerical simulation of thermo-hydro-mechanical coupling effect in mining fault-mode hot dry rock geothermal energy. Renewable Energy 2019, 139: 120-135.

Xu, T., Sonnenthal, E., Spycher, N., et al. TOUGHREACT user's guide: A simulation program for non-isothermal multiphase reactive geochemical transport in variable saturated geologic media. Lawrence Berkeley National Lab.(LBNL), Berkeley, CA (United States), 2004.

Yao, J., Zhang, X., Sun, Z., et al. Numerical simulation of the heat extraction in 3D-EGS with thermal-hydraulic-mechanical coupling method based on discrete fractures model. Geothermics 2018, 74: 19-34.

Yu, C., Lei, S., Yang, C., et al. Scenario analysis on operational productivity for target EGS reservoir in I-lan area, Taiwan. Geothermics 2018, 75: 208-219.

Zeng, Y., Su, Z., Wu, N. Numerical simulation of heat production potential from hot dry rock by water circulating through two horizontal wells at Desert Peak geothermal field. Energy 2013, 56: 92-107.

Zeng, Y., Wu, N., Su, Z., et al. Numerical simulation of heat production potential from hot dry rock by water circulating through a novel single vertical fracture at Desert Peak geothermal field. Energy 2013, 63: 268-282.